ChemComm

Accepted Manuscript

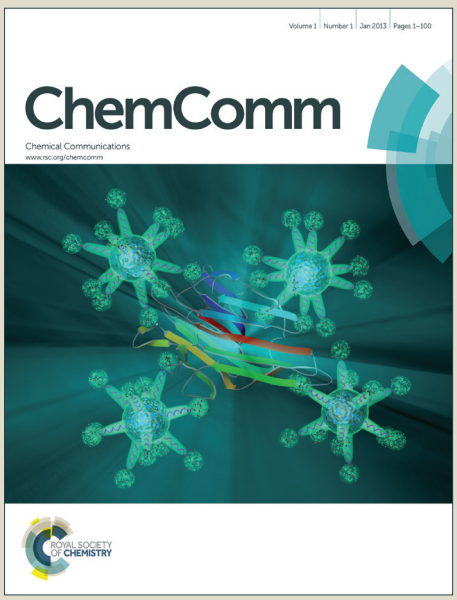

ROYAL SOCIETY OF CHEMISTRY

www.rsc.org/chemcomm

Journal Name

RSCPublishing

COMMUNICATION

High Performance Full Color OLEDs based on a Class of Molecules with Dual Carrier Transport Channels and Small Singlet-Triplet Splitting

Chenglong Li, Shipan Wang, Weiping Chen, Jinbei Wei, Guochun Yang, Kaiqi Ye, Yu Liu,* and Yue Wang*

Cite this: DOI: 10.1039/x0xx00000x

Received 00th January 2015,
Accepted 00th January 2015

DOI: 10.1039/x0xx00000x

www.rsc.org/

Two deep blue emitting materials **PPI-PPITPA** and **PPI-PPIPCz** with dual carrier transport property and small singlet-triplet splitting feature are designed and synthesized. **PPI-PPITPA** and **PPI-PPIPCz** not only were used as non-doped emitting layer to fabricate highly efficient deep blue OLEDs, but also as hosts to construct high performance green, yellow and red phosphorescent OLEDs.

Organic light-emitting devices (OLEDs) are of current interest from both scientific and practical points of view due to their applications in the next generation full-color flat-panel displays and solid-state lighting sources.[1] Generally, fine quality full-color displays or white color lighting sources are constructed by rational combination of high performance deep blue (**B**), green (**G**), yellow (**Y**) and red (**R**) emitters together with different host materials.[2] Therefore, achieving high performance **R**, **Y**, **G** and **B** electroluminescence (EL) based on simple material system with an aim to minimize the manufacture cost of materials and simplify the fabrication process is an important issue for OLED applications. In principle, a deep blue emitting material with balanced carrier transport characteristic and relatively high triplet energy (E_T) may be employed as an efficient host for **G**, **Y** and **R** phosphorescent emitters, simultaneously. The high E_T enables **G**, **Y** and **R** phosphors to harvest the triplet energy of blue emitter. However, the high performance non-doped blue electroluminescent materials are usually not suitable hosts for phosphorescent OLEDs (PhOLEDs) due to their low E_T and poor carrier transport property.[3] On the other hand, the efficient hosts for **G**, **Y** and **R** phosphors often displayed low efficiency when they were used as emitters in blue color OLEDs.[4] So far, it is still a challenge to achieve highly efficient full color OLEDs based on a deep blue emitting material.

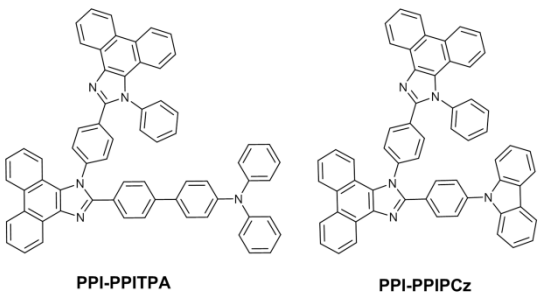

Figure 1. Molecular strucutres of **PPI-PPITPA** and **PPI-PPIPCz**.

To gain the multi-functional organic materials, which can be used not only as emitters to fabricate highly efficient deep blue OLEDs, but also as hosts to construct highly efficient **G**, **Y** and **R** OLEDs, we proposed the molecular design and synthesis strategy as following: (**i**) the molecules are supposed to have hole transport moiety (donor) and electron transport moiety (acceptor) with high photoluminescent (PL) quantum yield (Φ_{PL}) in solid state; (**ii**) the electron transport moieties and the hole transport moieties should be able to separately assemble together to form electron and hole transport channels, respectively, in solid state; (**iii**) to obtain deep blue emission, the donor-acceptor (D-A) molecule should have relatively weak charge transfer property since strong D-A structure

State Key Laboratory of Supramolecular Structure and Materials, College of Chemistry, Jilin University, Changchun 130012, P. R. China. E-mails: yuliu@jlu.edu.cn (Y. Liu); yuewang@jlu.edu.cn (Y. Wang); Fax: +86-431-85193421; Tel: +86-431-85168484 .

† Electronic Supplementary Information (ESI) available: Synthetic procedures and characterization data; DFT calculation result of PPI-PPIPCz, CV curves, TGA, DSC, Energy level diagram and CCDC 1058058; See DOI: 10.1039/c000000x/

can induce red shifted emission; (**iv**) the singlet-triplet splitting (ΔE_{ST}) should be quite small to ensure the triplet excited state energy is high enough to excite **G** phosphorescent dopant. In this communication, we report two organic molecules (**PPI-PPITPA** and **PPI-PPIPCz**) composed of two phenyl-phenanthroimidazol (**PPI**) and one triphenylamine (**TPA**) or phenyl-carbazole (**PCz**) groups (**Figure 1**). Using **PPI-PPITPA** and **PPI-PPIPCz** as non-doped deep blue emitters and hosts for **G**, **Y** and **R** phosphorescent dopants, highly efficient full color OLEDs are fabricated.

PPI-PPITPA and **PPI-PPIPCz** are synthesized through a simple procedure (**Scheme S1**) and fully characterized by NMR, mass spectra, and element analyses (see **Supporting Information**). The **PPI-PPITPA** molecule displays a V-type geometry feature (**Figure S1**) as demonstrated by single-crystal X-ray analysis. The theoretically calculated molecular orbital distribution of **PPI-PPITPA** is shown in **Figures 2a** and **2b**. The HOMO orbital is totally localized at **PPITPA** group, while the LUMO orbital distributes on the **PPI** group and imidazole ring of **PPITPA**. The molecular orbital distribution of **PPI-PPIPCz** is similar to **PPI-PPITPA** (**Figure S2**). Obviously, the HOMO and LUMO of **PPI-PPITPA** and **PPI-PPIPCz** display adequate separation feature, which benefits the hole- and electron-transport (bipolar property) and reduction of the singlet-triplet splitting.[5] The molecular packing (**Figure 2c**) of **PPI-PPITPA** reveals that the **PPI** and **PPITPA** moieties separately aggregate into stack columns indicating that the electron and hole transport channels are perfectly constructed, respectively. Though stacking model in the film is different from that in single crystal, the current–voltage characteristics (**Figure S3**) of single carrier devices also verify that both compounds have bipolar transport ability. The **PPI** (LUMO) and **PPITPA** (HOMO) moieties individually undertake the electron and hole transport

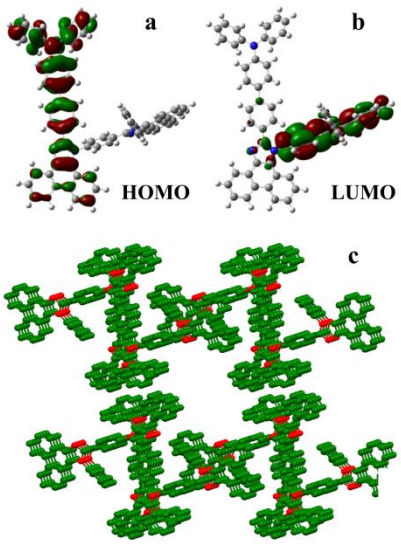

Figure 2. Calculated spatial distributions of the HOMO (a) and LUMO (b) and molecular packing (c) of **PPI-PPITPA**.

functions. The calculated electron (t_e) and hole (t_h) transfer integrals for **PPI-PPITPA** are 0.025 and 0.061 eV, respectively, suggesting that **PPI-PPITPA** can act as a bipolar transport material. The **PPI-PPITPA** shows clear reduction and oxidation waves (**Figure S4**), revealing that this molecule should have good electron and hole transport abilities. Both of the two compounds exhibit excellent thermal stability as evidenced by their high decomposition temperatures (corresponding to 5% weight loss) of 568 °C for **PPI-PPITPA** and 524 °C for **PPI-PPIPCz** (**Figure S5**). The glass-transition temperatures (T_g) are as high as 187 °C for **PPI-PPITPA** and 193 °C for **PPI-PPIPCz** (**Figure S6**). The distinguished thermal properties of the two compounds are favourable to form uniform thin films upon thermal evaporation, which are advantageous for application in OLEDs.

The photophysical properties of **PPI-PPITPA** and **PPI-PPIPCz** were analyzed by UV-vis and PL measurements (**Figure 3** and **Table S1**). In dilute CH_2Cl_2 solution, the two compounds exhibit intense violet to deep blue emission with high Φ_{PL} of 0.90 for **PPI-PPITPA** and 0.73 for **PPI-PPIPCz**. And the emission maximum of **PPI-PPIPCz** (402 nm) is much blue-shifted with respect to that of **PPI-PPITPA** (446 nm) in solution, which should be ascribed to the one more benzene ring in **PPI-PPITPA**, inducing an elongated conjugation. Interestingly, in the thin film state, **PPI-PPIPCz** shows similar emission band with **PPI-PPITPA**, peaking at around 450 nm. The Φ_{PL} of the thin films were measured to be 0.53 for **PPI-PPITPA** and 0.89 for **PPI-PPIPCz**. Such high fluorescence efficiencies are essential for high-efficiency deep blue OLEDs. Based on low-temperature PL measurements, the triplet energy levels are estimated to be 2.40 eV for **PPI-PPITPA** and 2.48 eV for **PPI-PPIPCz**, respectively, which are sufficiently high for the excitation of **GYR** phosphorescent dopants. The ΔE_{ST} values of PPI-PPITPA and PPI-PPIPCz were calculated to be 0.38 eV and 0.35 eV, respectively. The small ΔE_{ST} are advantageous for efficient energy transfer from the triplet excited state of hosts to **GYR** phosphorescent emitters.

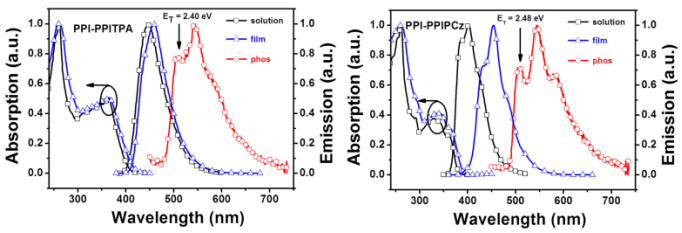

Figure 3. Room-temperature UV-vis absorption spectra, PL spectra of **PPI-PPITPA** and **PPI-PPIPCz** in CH_2Cl_2 solution and in neat films, as well as their phosphorescence spectra in thin film at 77 K.

We first examined the two compounds' EL property as blue emitters by fabricating non-doped OLEDs with a structure of [ITO/NPB (40 nm)/TCTA (5 nm)/**PPI-PPITPA** or **PPI-PPIPCz** (30 nm)/TPBI (50 nm)/LiF (1 nm)/Al] (device **B1** with emitting layer (EML) composed of **PPI-PPITPA** and device **B2** with EML composed of **PPI-PPIPCz**). The energy-level diagram and molecular structures of the used materials are shown in **Figure S7**. In devices **B1** and **B2**, we utilized NPB (4,4'-bis[N-(1-naphthyl)-N-phenyl amino] biphenyl) as the hole-transporting layer (HTL), TCTA (4,4',4''- tris(Ncarbazolyl)triphenylamine) as the exciton-blocking layer, TPBI (1,3,5-tris(*N*-phenylbenzimidazol-2-yl)benzene) as the electron-transporting layer (ETL) and hole-blocking layer. LiF served as electron-injecting layer and Al served as cathode. The non-

doped devices **B1** and **B2** exhibit deep-blue emission with CIE coordinates of (0.15, 0.08) and (0.15, 0.07), respectively, both of which are very close to the NTSC (National Television Standards Committee) blue standard (CIE: 0.14, 0.08) and remain almost unchanged over a wide range of driving voltage. As shown in **Figure 4** and **Figure S8**, the maximum external quantum efficiencies (EQEs) of Device **B1** and **B2** are 7.7% and 8.1%, respectively. Device **B1** using **PPI-PPITPA** as emitter shows a low turn-on voltage of 3.2 V and a maximum luminance of 13950 cd m^{-2} at 10.5 V. The maximum current (CE) and power (PE) efficiencies of this device are 5.6 cd A^{-1} and 5.5 lm W^{-1}, respectively. Device **B2** shows a similar performance. It turns on at 3.4 V and achieves a maximum brightness of 13820 cd m^{-2} at 10.5 V. The maximum CE and PE can be up to 4.8 cd A^{-1} and 4.5 lm W^{-1}. To the best of our knowledge, these efficiencies are the highest values reported for non-doped blue OLEDs with CIEy below 0.10.[6] Moreover, the EQE of these two devices maintains 5.4% and 6.0% respectively at a high brightness of 1000 cd m^{-2}, indicating relatively small efficiency roll-offs.

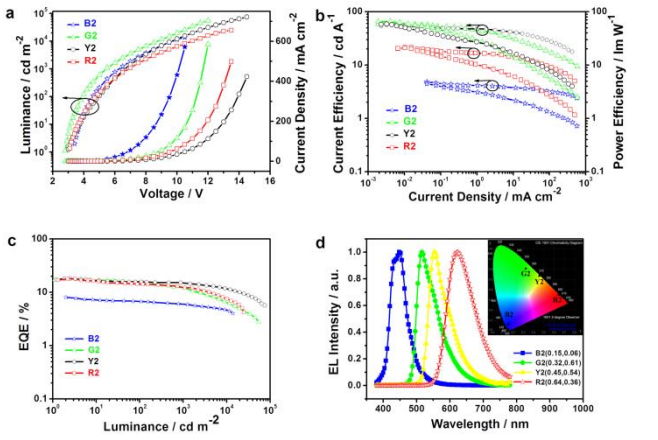

Figure 4. (a) Current density–voltage–brightness (*J–V–L*) characteristics; (b) Current efficiencies and power efficiencies versus current density curves; (c) External quantum efficiency versus luminance characteristics; (d) EL spectra and CIE1931 coordinates of devices **B2**, **G2**, **Y2** and **R2** based on **PPI-PPIPCz**.

The EQE of OLEDs can be expressed by the well-known equation of EQE = $\eta_{out} \times \eta_{rc} \times \eta_{\gamma} \times \Phi_{PL}$,[7] where η_{out} is the light-out-coupling efficiency (~20%), η_{rc} is the product of the charge recombination efficiency that is ideally 100% if holes and electrons are fully balanced and completely recombined to form excitons, η_{γ} is efficiency of radiative exciton production (25% for conventional fluorescent OLEDs), Φ_{PL} is photoluminescence (PL) quantum yield of the emitter molecules (0.53 for **PPI-PPITPA** and 0.89 for P**PI-PPIPCz)**. Thus, the maximum EQE values of **PPI-PPITPA** and **PPI-PPIPCz** devices can be calculated as 2.7% and 4.5%, respectively. Clearly, the obtained EQEs (7.7% for **PPI-PPITPA**, 8.1% for **PPI-PPIPCz)** overcome the theoretical EQE limit of 5% for the conventional fluorescent OLEDs. Since no delayed fluorescence was observed from transient PL (**Figure S8**), the high EQEs did not seem to be in accordance with TADF.[8] At this stage we cannot give precise explanation for this phenomena and detail experiments should be performed to disclose the mechanism.

To explore the potential applications of these two compounds as host materials for **G**, **Y** and **R** phosphorescent dopants, we fabricated **GYR** PhOLEDs with configurations of [ITO/NPB (40 nm)/TCTA (5 nm)/EML (30 nm)/TPBI (50 nm)/LiF (1 nm)/Al (100 nm)] (EML: **PPI-PPITPA**:5 wt% $Ir(ppy)_3$ for device **G1**, **PPI-PPITPA**:5 wt% $Ir(ppy)_2(dipig)$ for device **Y1**, **PPI-PPITPA**:8 wt% $Ir(MDQ)_2(acac)$ for device **R1** and **PPI-PPIPCz**:5 wt% $Ir(ppy)_3$ for device **G2**, **PPI-PPIPCz**:5 wt% $Ir(ppy)_2(dipig)$ for device **Y2**, **PPI-PPIPCz**:8 wt% $Ir(MDQ)_2(acac)$ for device **R2**). The green phosphorescent complex $Ir(ppy)_3$ is *fac*-tris(2-phenylpyridine) iridium(III), yellow complex $Ir(ppy)_2(dipig)$ is bis(2-phenylpyridinato)-N,N'-diisopropyl-diisopropyl- guanidinate iridium(III) and red complex $Ir(MDQ)_2(acac)$ is bis(2-methyldibenzo-[*f*,*h*]quinoxaline) acetylacetonate iridium(III) (Figure **S9**).

Figure 4 and **Figure S8** present the current density–voltage–brightness (*J–V–L*) characteristics, device performances and EL spectra of the devices. The EL spectra are identical to the PL spectra (**Figure S10**) of the doped thin films. Device **G2** exhibits a low turn-on voltage of 2.8 V. The maximum EQE of 17.8% and PE of 65.7 lm W^{-1} are among the best values for green phosphorescent OLEDs with blue emitters as hosts.[9] However, device **G1** shows a much lower EL efficiency than device **G2.** The reason can be attributed to the lower triplet energy level (E_T = 2.40 eV) of **PPI-PPITPA**, which may cause back energy transfer from the green guest triplet states to the host, resulting in a loss in efficiency. Yellow PhOLEDs with excellent performance were also achieved by employing these two compounds as hosts. For instance, devices **Y1** exhibits the maximum EQE of 19.1%, CE of 61.8 cd A^{-1}, and PE of 65.5 lm W^{-1}, and device **Y2** shows the similar behavior with the maximum EQE of 18.1%, CE of 56.5 cd A^{-1}, and PE of 58.8 lm W^{-1}. Finally, deep red PhOLEDs were fabricated by using **PPI-PPITPA** and **PPI-PPIPCz** as host. Device **R2** exhibits the maximum luminance of 24810 cd m^{-2} at 13.5 V and excellent EL efficiencies (18.0%, 21.3 cd A^{-1}, and 20.9 lm W^{-1}), whereas device **R1** exhibits the maximum luminance of 18020 cd m^{-2} at 11.0 V and EL efficiencies (16.8%, 19.8 cd A^{-1}, and 21.5 lm W^{-1}) (**Figure 4** and **Figure S8**). The PE values of devices **R1** and **R2** are comparable to recently reported highly efficient deep red PhOLEDs.[10] Above experimental results demonstrates that **PPI-PPITPA** and **PPI-PPIPCz** are universal host materials for **GYR** phosphorescent emitters. The detail EL parameters of the **RYGB** OLEDs are summarized in **Table 1**.

In conclusion, we have designed and synthesized two deep blue emitting materials **PPI-PPITPA** and **PPI-PPIPCz** with dual carrier transport property and small singlet-triplet splitting feature. The single crystal study of **PPI-PPITPA** revealed that the **PPI** and **PPITPA** moieties assemble into electron and hole transport channels, respectively, in solid state. The strong deep blue emission and good ambipolar carrier transport characteristics of **PPITPA** and **PPI-PPIPCz** ensure that the OLEDs with the two compounds as non-dopant EML display extremely high EQE of 7.7%, 8.1% with true deep blue CIE (0.15, 0.08) and (0.15, 0.07). Furthermore, the small singlet-triplet splitting and good carrier transport properties allow **PPITPA** and **PPI-PPIPCz** as hosts to fabricate **RYG** phosphorescent emitting layers for PhOLEDs. High performance **G**, **Y** and **R** PhOLEDs with EQE of 17.8%, 18.1% and 18.0%,

respectively, have been successfully obtained based on the two compounds and phosphors. These results demonstrate an efficient strategy to achieve full color OLEDs by developing the deep blue organic luminescent materials with ideal **D-A** molecular structure and molecular packing in solid state as well as small singlet-triplet splitting.

Table 1. Electroluminescent performances of the devices.[a)]

Device	Dopant	V_{on}/V	L_{max}/cd m^{-2}	CE[b)]/cd A^{-1}	PE[b)]/lm W^{-1}	EQE[b)]/%	CIE (*x*,*y*)[c)]
B1	no	3.2	13950	5.6, 4.6, 3.9	5.5,3.2,2.0	7.7, 6.4, 5.4	0.15, 0.08
B2	no	3.4	13820	4.8, 4.1, 3.6	4.5, 2.8, 1.8	8.1, 6.8, 6.0	0.15, 0.07
G1	$Ir(ppy)_3$	2.8	7022	26.6, 11.5, 3.7	29.9, 8.3, 1.5	7.9, 3.5, 1.0	0.32, 0.60
G2	$Ir(ppy)_3$	2.8	55020	60.6, 51.5, 41.6	65.7, 41.9, 24.2	17.8, 15.3, 12.4	0.32, 0.61
Y1	$Ir(ppy)_2$(dipig)	2.9	68990	61.8, 55.5, 50.7	65.5, 37.6, 24.7	19.1, 17.2, 15.8	0.46, 0.53
Y2	$Ir(ppy)_2$(dipig)	3.0	75350	56.5, 49.7, 46.6	58.8, 32.2, 23.7	18.1, 15.8, 15.1	0.45, 0.54
R1	$Ir(MDQ)_2$(acac)	2.8	18020	19.8, 18.3, 16.3	21.5, 14.1, 10.1	16.8, 15.6, 13.8	0.64,0.36
R2	$Ir(MDQ)_2$(acac)	2.3	39138	21.3, 16.9, 14.8	20.9, 11.2, 6.7	18.0, 14.2, 12.4	0.64,0.36

[a)] Abbreviation: V_{on}: Turn-on voltage. L_{max}: Maximum luminance. CE: The maximum current efficiency. PE: The maximum power efficiency. EQE: The maximum external quantum efficiency. [b)] in the order of maximum, then values at 100 and 1000 cd m^{-2}. [c)] Measure at 100 cd m^{-2}.

C. L. Li and S. P. Wang contributed equally to this work. This work was supported by Natural Science Foundation of China (91333201 and 21221063), National Basic Research Program of China (2015CB655000) and Program for Chang Jiang Scholars and Innovative Research Team in University (No.IRT13018).

Notes and references

1 (a) M. A. Baldo, M. E. Thompson, S. R. Forrest, *Nature*, 2000, **403**, 750; (b) S. Reineke, F. Lindner, G. Schwartz, N. Seidler, K. Walzer, B. Lüssem, K. Leo, *Nature*, 2009, **459**, 234; (c) A. C. Grimsdale, K. L. Chan, R. E. Martin, P. G. Jokisz, A. B. Holmes, *Chem, Rev.*, 2009, **109**, 897; (d) W. C. H. Choy, W. K. Chan, Y. Yuan, *Adv. Mater.*, 2014, **26**, 5368; (e) T. Fleetham, G. Li, L. Wen, J. Li, *Adv. Mater.*, 2014, **26**, 7116.

2 (a) S. Chen, G. Tan, W-Y. Wong, H-S. Kwok, *Adv. Funct. Mater.*, 2011, **21**, 3785; (b) G. M. Farinola, R. Ragni, *Chem. Soc. Rev.*, 2011, **40**, 3467; (c) B. P. Yan, C. C. C. Cheung, S. C. F. Kui, H. F. Xiang, V. A. L. Roy, S. J. Xu, C. M. Che, *Adv. Mater.*, 2007, **19**, 3599; (d) H. Sasabe, J. I. Takamatsu, T. Motoyama, S. Watanabe, G. Wagenblast, N. Langer, O. Molt, E. Fuchs, C. Lennartz, J. Kido, *Adv. Mater.*, 2010, **22**, 5003; (e) R. J. Wang, D. Liu, H. C. Ren, T. Zhang, H. M. Yin, G. Y. Liu, J. Y. Li, *Adv. Mater.*, 2011, **23**, 2823; (f) K. T. Kamtekar, A. P. Monkman, M. R. Bryce, *Adv. Mater.*, 2010, **22**, 572; (g) M. C. Gather, A. Köhnen, K. Meerholz, *Adv. Mater.*, 2011, **23**, 233; (h) C. Han, Z. Zhang, H. Xu, J. Li, G. Xie, R. Chen, Y. Zhao, W. Huang, *Angew. Chem. Int. Ed.*, 2012, **51**, 10104; (i) C. Fan, L. Zhu, T. Liu, B. Jiang, D. Ma, J. Qin, C. Yang, *Angew. Chem. Int. Ed.*, 2014, **53**, 2147.

3 (a) W. Y. Lai, Q. Y. He, R. Zhu, Q. Q. Chen, W. Huang, *Adv. Funct. Mater.*, 2008, **18**, 265; (b) L. Wang, Y. Jiang, J. Luo, Y. Zhou, J. H. Zhou, J. Wang, J. Pei, Y. Cao, *Adv. Mater.*, 2009, **21**, 4854; (c) L. Xiao, Z. Chen, B. Qu, J. Luo, S. Kong, Q. Gong, J. Kido, *Adv. Mater.*, 2011, **23**, 926; (d) C.-G. Zhen, Y.-F. Dai, W.-J. Zeng, Z. Ma, Z.-K. Chen, J. Kieffer, *Adv. Funct. Mater.*, 2011, **21**, 699.

4 (a) K. Wang, F. C. Zhao, C. G. Wang, S. Y. Chen, D. Chen, H. Y. Zhang, Y. Liu, D. G. Ma, Y. Wang, *Adv.Funct. Mate.*, 2013, **23**, 2672; (b) K. Wang, S. P. Wang, J. B. Wei, S. Y. Chen, D. Liu, Y. Liu, Y. Wang, *J. Mater. Chem. C.*, 2014, **2**, 6817.

5 (a) L. Duan, J. Qiao, Y. D. Sun, Y. Qiu, *Adv. Mater.*, 2011, **23**, 1137; (b) C.-J. Zheng, J. Wang, J. Ye, M. -F. Lo, X.-K. Liu, M.-K. Fung, X.-H. Zhang, C.-S. Lee, *Adv. Mater.*, 2013, **25**, 2205; (c) D. D. Zhang, L. Duan, Y. L. Li, H. Y. Li, Z. Y. Bin, D. Q. Zhang, J. Qiao, G. D. Dong, L. D. Wang, Y. Qiu, *Adv. Funct. Mater.*, 2014, **24**, 3551.

6 (a) W. J. Li, Y. Y. Pan, R. Xiao, Q. M. Peng, S. T. Zhang, D. G. Ma, F. Li, F. Z. Shen, Y. H. Wang, B. Yang, Y. G. Ma, *Adv. Funct. Mater.*, 2013, **24**, 1609; (b) R. Kim, S. Lee, K. H. Kim, Y. J. Lee, S. K. Kwon, J. J. Kim and Y. H. Kim, *Chem. Commun.*,2013, **49**, 4664; (c) J. N. Moorthy, P. Venkatakrishnan, D. F. Huang, T. J. Chow, *Chem. Commun.*, 2008, 2146-2148.

7 V. Jankus, C. -J. Chiang, F. Dias, A. P. Monkman, *Adv. Mater.*,2013, **25**, 1455.

8 (a) H. Uoyama, K. Goushi, K. Shizu, H. Nomura, C. Adachi, *Nature*, 2012, **492**, 234; (b) Q. Zhang, J. Li, K. Shizu, S. Huang, S. Hirata, H. Miyazaki, C. Adachi, *J. Am. Chem. Soc.*, 2012, **134**, 14706; (c) S. Y. Lee, T. Yasuda, Y. S. Yang, Q. Zhang, C. Adachi, *Angew. Chem. Int. Ed.*, 2014, **53**, 6402; (d) J. W. Sun, J. -H. Lee, C. -K. Moon, K. -H. Kim, H. Shin, J. -J. Kim, *Adv. Mater.*, 2014, **26**, 5684; (e) D. Zhang, L. Duan, C. Li, Y. Li, H. Li, D. Zhang, Y. Qiu, *Adv. Mater.*, 2014, **26**, 5050; (f) X. K. Liu, Z. Chen, C. J. Zheng, M. Chen, W. Liu, X. H. Zhang, C. S. Lee, *Adv. Mater.*, 2015, DOI: 10.1002/adma.201500013.

9 (a) H. H. Chou, C. H. Cheng, *Adv. Mater.*, 2010, **22**, 2468; (b) S.-J. Su, C. Cai and J. Kido, *Chem. Mater.*, 2011, **23**, 274; (c) S. L. Gong, Y. H. Chen, J. J. Luo, C. L. Yang, C. Zhong, J. G. Qin, D. G. Ma, *Adv. Funct. Mater.*, 2011, **21**, 1168; (d) X. K. Liu, C. J. Zheng, M. F. Lo, J. Xiao, C. S. Lee, M. K. Fungc, X. H. Zhang, *Chem. Commun.*, 2014, **50**, 2027; (e) P.-I. Shih, C.-H. Chien, F.-I. Wu, C.-F. Shu , *Adv. Funct. Mater.*, 2007, **17**, 3514.

10 (a) Y. Tao, Q. Wang, Y. Shang, C. L. Yang, L. Ao, J. Qin, D. G. Ma, Z. Shuai, *Chem. Commun.*, 2009, 77; (b) H. Sasabe , T. Chiba , S.-J. Su , Y. J. Pu , K. I. Nakayama . J. Kido, *Chem. Commun.*, 2008, 5821; (c) F. M. Hsu, C. H. Chien, Y. J. Hsieh, C. H. Wu, C. F. Shu, S. W. Liu, C. T. Chen, *J. Mater. Chem.*, 2009, **19**, 8002; (d) C. H. Chen, L. C. Hsu, P. Rajamalli, Y. W. Chang, F. L. Wu, C. Y. Liao, M. J. Chiu, P. Y. Chou, M. J. Huang, L. K. Chu, C. H. Cheng, *J. Mater. Chem. C.*, 2014, **2**, 6183; (e) C. H. Fan, P. P. Sun, T. H. Su, C. H. Cheng, *Adv. Mater.*, 2011, **23**, 2981.

